Investigation of runaway electrons in the current ramp-up by a fully non-inductive lower hybrid current drive on the EAST tokamak

2013 Phys. Scr. 87 055504

(http://iopscience.iop.org/1402-4896/87/5/055504)

Phys. Scr. **87** (2013) 055504 (6pp) doi:10.1088/0031-8949/87/05/055504

Investigation of runaway electrons in the current ramp-up by a fully non-inductive lower hybrid current drive on the EAST tokamak

H W Lu[1,2], X J Zha[1,2], F C Zhong[1,2], L Q Hu[3], R J Zhou[3] and EAST Team

[1] Department of Applied Physics, Donghua University, Shanghai 201620, People's Republic of China
[2] Member of Magnetic Confinement Fusion Research Center, Ministry of Education, People's Republic of China
[3] Institute of Plasma Physics, Chinese Academy of Sciences, Hefei 230031, People's Republic of China

E-mail: hwlu@dhu.edu.cn

Received 21 January 2013
Accepted for publication 19 March 2013
Published 17 April 2013
Online at stacks.iop.org/PhysScr/87/055504

Abstract
The possibility of using a lower hybrid wave (LHW) to ramp up the plasma current (I_p) from a low level to a high enough level required for fusion burn in the EAST (experimental advanced superconducting tokamak) tokamak is examined experimentally. The focus in this paper is on investigating how the relevant plasma parameters evolve during the current ramp-up (CRU) phase driving by a lower hybrid current drive (LHCD) with poloidal field (PF) coil cut-off, especially the behaviors of runaway electrons generated during the CRU phase. It is found that the intensity of runaway electron emission increases first, and then decreases gradually as the discharge goes on under conditions of PF coil cut-off before LHW was launched into plasma, PF coil cut-off at the same time as LHW was launched into plasma, as well as PF coil cut-off after LHW was launched into plasma. The relevant plasma parameters, including H_α line emission (Ha), impurity line emission (UV), soft x-ray emission and electron density n_e, increase to a high level. The loop voltage decreases from positive to negative, and then becomes zero because of the cut-off of PF coils. Also, the magnetohydrodynamic activity takes place during the CRU driving by LHCD.

PACS numbers: 52.38.Ph, 52.55.Wq

(Some figures may appear in colour only in the online journal)

1. Introduction

In tokamak plasmas, because of the decrease of the Coulomb collision frequency with energy, electrons with energy larger than some critical value are continuously accelerated by the toroidal electric field, i.e., they run away [1]. It is widely accepted that runaway electrons are generated via two mechanisms. Primary (or Dreicer) generation happens via a diffusion process in velocity space [2, 3]. Secondary (or avalanche) generation occurs when runaway electrons kick thermal electrons past the critical energy and turn them into runaway electrons [4]. In fusion devices, especially the disruptions, these runaway electrons can reach energies in excess of 100 MeV and they can damage the wall of the vacuum vessel when they hit it in large numbers [5]. Reducing the energy of runaway electrons and the mitigation of their effects is a key issue for the International Thermonuclear Experimental Reactor (ITER) [6–10] during fast plasma shutdowns and disruptions.

The main heating phase is usually carried out at high plasma current, since in a tokamak high current means high confinement. This current is ramped up from a negligible value just after the plasma breakdown to a plateau value, usually mainly by inductive means [11]. Initiation and ramp-up of plasma discharges without a central solenoid (or a much reduced one) provides distinct advantages for burning

plasma devices, especially in the engineering design and cost [12]. Key parts of the ITER scenarios are determined by the capability of the proposed poloidal field (PF) coil set. They include the plasma breakdown at low loop voltage, the current rise phase, the performance during the flat top phase and a ramp-down of the plasma [13]. A significant amount of magnetic flux is needed to ramp the plasma up inductively; thus the flux consumption during the current ramp is also a key element in the design of the PF system [11].

Simulations and experiments are focused on 15 MA scenarios for ITER [14], being the most challenging of the ITER reference scenarios for the superconducting PF coils. In the course of producing suitable plasma configurations at 15 MA in ITER, with sufficient wall clearance and control over the divertor strike point positions, the PF coils must remain within several limits, such as coil current, coil field, voltage, power and central solenoid force limits [13]. ASDEX Upgrade and Tore Supra [15] developed, for the first time, operation without resistor switches in the ohmic heating circuits. Several superconducting tokamaks contributed to these studies (Tore Supra, EAST [16] and KSTAR [17]). Finally, the confinement/magnetohydrodynamic (MHD) properties of the final 'main heating' phase depend on the q-profile obtained at the end of the ramp-up and may be optimized by applying additional heating and a non-inductive current drive during the current ramp [11]. The lower hybrid wave (LHW) has been shown to drive plasma current efficiently in current ramp-up (CRU), flat top and current ramp-down phase, both theoretically [18, 19] and experimentally [20, 21].

The possibility of using the LHW to ramp up the plasma current (I_p) from a low level to a high enough level required for fusion burn in the EAST (experimental advanced superconducting tokamak) tokamak is examined experimentally. Current ramps are characterized by large changes in almost all the relevant plasma parameters as the current is varied. In addition, the two ramps are not symmetric at the same current level, as for example the ohmic heating power is large and peaked off-axis in the ramp-up but small and peaked on-axis in the ramp-down. [22]. There are several issues to be addressed during plasma current ramp phases of tokamak operation: MHD activity can take place and lead to early plasma termination, depending on the shape of the plasma current density profile [11]. The focus in this paper is on investigating how the relevant plasma parameters evolve during the CRU phase driving by a lower hybrid current drive (LHCD) with PF coil cut-off, especially the behaviors of runaway electrons generated during the CRU phase.

2. PF coil cut-off before LHW was launched into plasma

The EAST tokamak is a fully superconducting tokamak in both toroidal field (TF) and PF with non-circular cross section. It has a major radius of $R_0 = 1.75$ m, a minor one of $a = 0.4$ m, with an aspect ratio of 4.25, an elongation rate of 1.2–2, and multi-configurations of single-null divertor, double-null divertor and circular configurations with a limiter [23]. The superconducting TF magnetic system of EAST consists of a toroidal array of 16 coils. It produces a 3.5 T TF at the plasma major radius of 1.7 m. The superconducting PF system of EAST consists of 12 coils located symmetrically above the vertical mid-plane and the equatorial plane. The PF coils provide a 1.0 MA ohmic plasma current with up to 11 V s of inductive flux [24, 25].

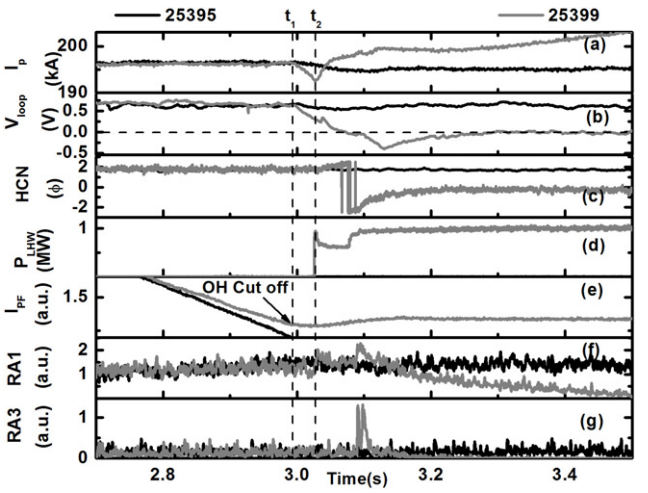

Figure 1. Time evolution of the main plasma parameters for the discharge with CRU by LHCD only (No. 25399) and normal ohmic discharge (No. 25395). From top to bottom: the plasma current (I_P), loop voltage (V_{loop}), far infrared laser interferometer (HCN), LHCD power (P_{LHW}), PF coil current (I_{PF}), hard x-ray emission in 0.1–1.1 MeV detected by the CdTe detector (RA1), hard x-ray emission in 0.5–7.0 MeV detected by the NaI(TL) detector (RA3).

In figure 1 we show the time evolution of the main plasma parameters for the discharge with CRU by LHCD without resistor switches in the ohmic heating circuits (No. 25399) and normal ohmic discharge (No. 25395). The plasma current is fixed at about 195 kA. The line integral electron density is maintained at about $n_e l = 1.6 \times 10^{19}$ m^{-2}. We can see from figure 1 that the solenoidal current cut off at $t_1 = 2992$ ms. Hold solenoidal current flat from $t_1 = 2992$ ms on. A 1 MW LHW was launched into plasma 35 ms later (from $t_2 = 3027$ ms on) in order to drive plasma current. The plasma current decays from 195 kA to 192 kA within 4 ms (from $t_1 = 2992$ ms to $t_2 = 3027$ ms) as a result of the ohmic heating cut-off and ramps up because of the LHCD after PF coil current cut-off. A fully non-inductive LHCD is being applied. The plasma current is ramped up in 500 ms from 192 to 207 kA. I_p ramp-up to over 15 kA was achieved by LHW only. The inductive loop voltage was produced by changing solenoidal current in ohmic heated plasmas, while the loop voltage was produced by plasma current decays when the PF coil current cut off as shown in figure 1.

The hard x-ray (HXR) emission resulting from the thick target bremsstrahlung when runaway electrons are lost from the plasma and impinge on the vessel walls or plasma facing components [26] provides information on generation, loss and energy content of the runaway electrons [27–29]. We can see from figure 1 that the hard x-ray emission in 0.1–1.1 MeV and in 0.5–7.0 MeV decreases in the CRU phase. Therefore, we can deduce that the runaway electrons decrease during the CRU with LHCD.

Figure 2 shows the time evolution of the main plasma radiation parameters for discharges No. 25399 (CRU with LHCD only) and No. 25395 (normal ohmic discharge).

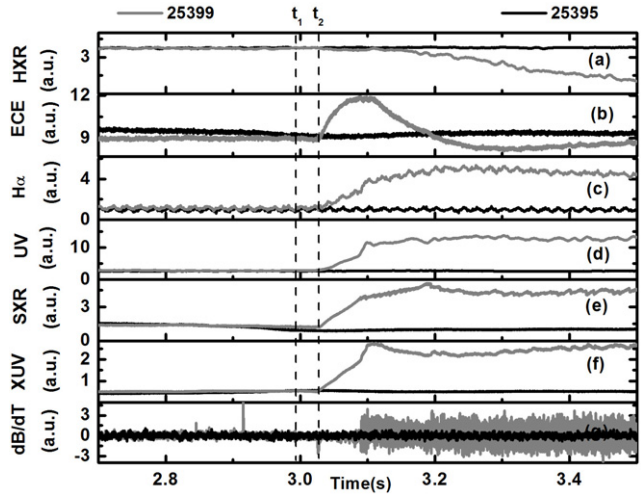

Figure 2. Time evolution of the main plasma radiation parameters for discharges No. 25399 (CRU with LHCD only) and No. 25395 (normal ohmic discharge). From top to bottom: hard x-ray emission produced by fast electron bremsstrahlung (HXR), ECE, H_α line emission (Ha), impurity-CIII line-emission intensity (UV), soft x-ray emission detected by photodiode array (SXR), plasma radiation loss detected by absolute XUV, Mirnov oscillations detected by Mirnov probes ($\mathrm{d}B/\mathrm{d}T$).

From figure 2 we can see that the hard x-ray emission produced by fast electron bremsstrahlung decreases because of the decrease of the acceleration by loop voltage. Electron cyclotron emission (ECE) increases to a high level from $t_2 = 3027$ ms when LHW was launched into plasma and ECE begins to decrease to a lower level from $t = 3100$ ms. The reason is that a lot of super-thermal electrons produce because LHW was launched into plasma. Furthermore, the positive loop voltage (from $t_1 = 2992$ ms to $t = 3100$ ms, $V_{\mathrm{loop}} > 0$) induced by decay of plasma current can accelerate electrons. Therefore, ECE emission increases to a high level from $t_2 = 3027$ ms to $t = 3100$ ms. And then ECE emission decays because of the increased line integral electron density and the negative loop voltage as shown in figure 1. From figure 2 we can see that H_α line emission (Ha), impurity line emission (UV) and soft x-ray emission increase. Therefore, the plasma radiation loss detected by absolute extreme ultraviolet photodiode (XUV) increases to a very high level because of extensive impurity emission. Also, the MHD activity takes place during the CRU driving by LHCD.

Figure 3 shows the time evolution of the low-energy hard x-ray (0.3–1.0 MeV) counts together with plasma current for shots No. 25395 and No. 25399. From figure 3 we can see that the low-energy runaway electron (0.3–1.0 MeV) counts increase when LHW was launched into plasma, and then decrease gradually as the discharge goes on.

Time evolution of the high-energy hard x-ray (0.5–7.0 MeV) counts together with plasma current for shots No. 25395 and No. 25399 is shown in figure 4. From figure 4 we can see that the high-energy runaway electron (0.5–7.0 MeV) counts increase after LHW was launched into plasma, and then decrease gradually as the discharge goes on, which is similar to the low-energy runaway electrons shown in figure 3.

The reason is that the positive loop voltage of shot No. 25399 decreases to negative because of ohmic heating

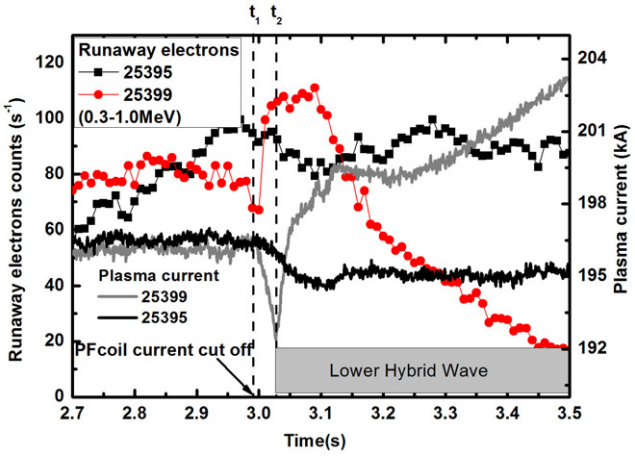

Figure 3. Time evolution of the low-energy hard x-ray emission (0.3–1.0 MeV) counts together with plasma current for shots No. 25395 and No. 25399.

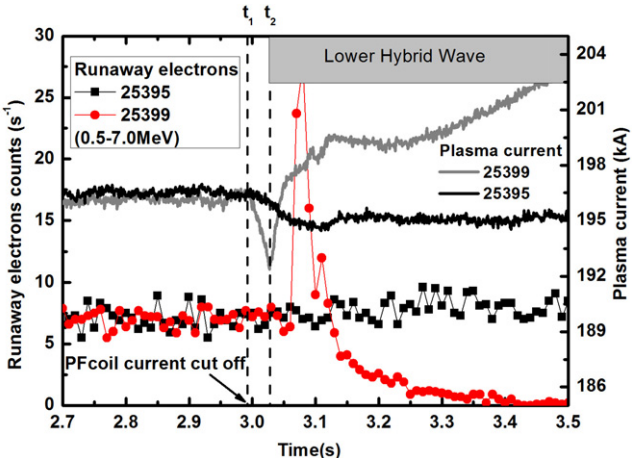

Figure 4. Time evolution of the high-energy hard x-ray emission (0.5–7.0 MeV) counts together with plasma current for shots No. 25395 and No. 25399.

cut-off, and then loop voltage remains about zero when a fully non-inductive LHCD is being applied which is shown in figure 1. Furthermore, the line integral electron density of shot No. 25399 increased after LHW was launched into plasma because of extensive impurity emission. These can be understood well by the Dreicer process [30]. Runaway is caused by collisional diffusion of electrons in velocity space to velocities higher than a critical one, above which the electric force overcomes the frictional force due to collisions [31]. The critical velocity ($v_{\mathrm{c}}^2 = \frac{3ne^3 \ln\Lambda}{4\pi\varepsilon_0^2 m_{\mathrm{e}} E}$, as is shown in [32]) increases with the electron density n_{e}, and decreases with the electric field E. So the number of electrons accelerating to the critical velocity decreases with increasing electron density, and decreasing loop voltage. That is to say the increase of electron density and the decrease of loop voltage will reduce the production of runaway electrons, which determine the intensity of HXR emission.

Figure 5 shows the time evolution of hard x-ray emission in several energy intervals detected by the CdTe detector for shot No. 25399. From the figure we can see that the counts of hard x-ray emission in 70–140 keV reduce from 3×10^4 to $4 \times 10^3\ \mathrm{s}^{-1}$, more than 80%. The counts of hard x-ray emission in every energy interval in 70–1070 keV reduce to a very low level.

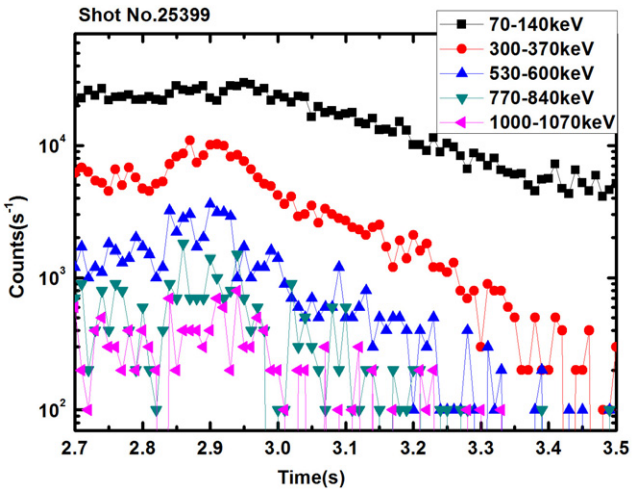

Figure 5. Time evolution of hard x-ray emission in several energy intervals detected by the CdTe detector for shot No. 25399.

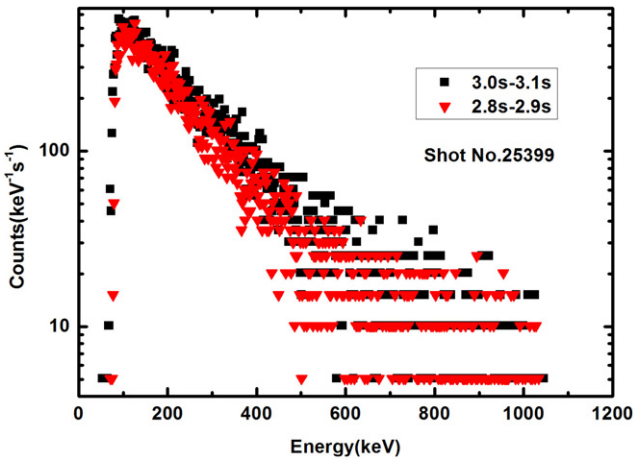

Figure 6. Spectrum of hard x-ray emission during 2.8–2.9 and 3.0–3.1 s detected by the CdTe detector for shot No. 25399.

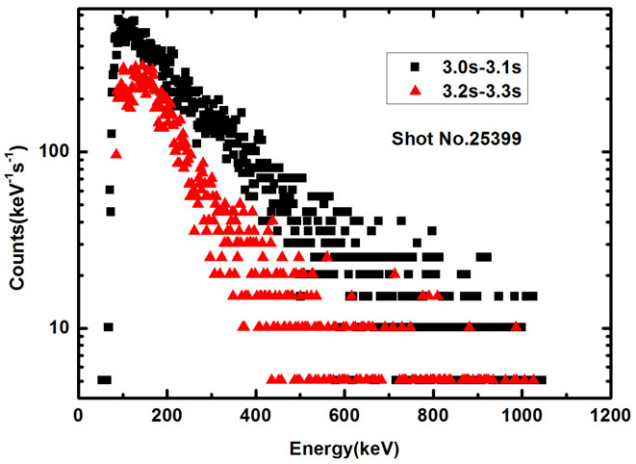

Figure 7. Spectrum of hard x-ray emission during 3.0–3.1 and 3.2–3.3 s detected by the CdTe detector for shot No. 25399.

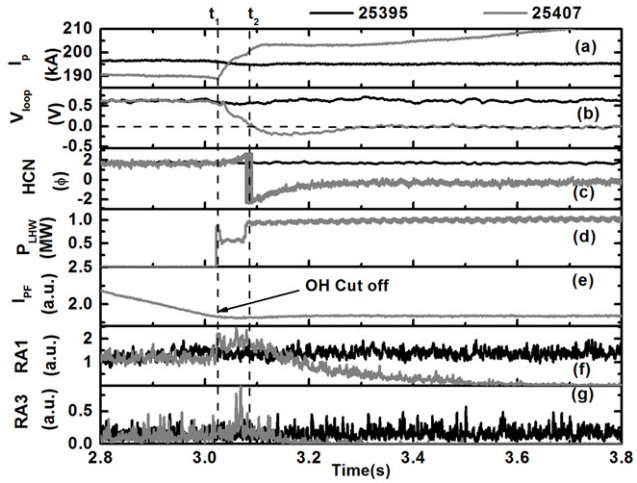

Figure 8. Time evolution of the main plasma parameters for the discharge with CRU by LHCD only (No. 25407) and normal ohmic discharge (No. 25395). From top to bottom: the plasma current (I_P), loop voltage (V_{loop}), far infrared laser interferometer (HCN), LHCD power (P_{LHW}), PF coil current (I_{PF}), hard x-ray emission in 0.1–1.1 MeV detected by the CdTe detector (RA1), hard x-ray emission in 0.5–7.0 MeV detected by the NaI(TL) detector (RA3).

Figures 6 and 7 show the spectrums of hard x-ray emission during 2.8–2.9, 3.0–3.1 and 3.2–3.3 s detected by the CdTe detector for shot No. 25399. The discharge is normally ohmic plasmas during 2.8–2.9 s. The PF coil current cut-off and LHW was launched into plasmas during 3.0–3.1 s. Plasma current is ramped up by a fully non-inductive LHCD with PF coil cut-off during 3.2–3.3 s. From figure 6 we can see that the counts of each energy interval of hard x-ray emission during 3.0–3.1 s are a little more than that during 2.8–2.9 s, while we can see from figure 7 that the counts of each energy interval of hard x-ray emission during 3.2–3.3 s are much lower than that during 3.0–3.1 s.

3. PF coil cut-off at the same time as LHW was launched into plasma

Figure 8 shows the time evolution of the main plasma parameters for the discharge with CRU by LHCD only (No. 25407) and normal ohmic discharge (No. 25395). From figure 8 we can see that PF coil current cut off at about $t_1 = 3022$ ms. At the same time 1 MW LHW was launched into plasma to ramp up plasma current only, instead of ohmic heating. The intensity of lower energy (0.3–1.0 MeV) hard x-ray emission during $t_1 = 3022$ ms and $t_2 = 3087$ ms is stronger than that during 2.8–3.0 s. The reason is that the loop voltage cannot reduce to zero immediately because of the electromagnetic induction. The LHW can drive fast electrons which can also be accelerated by loop voltage. When the velocity of fast electrons becomes larger than the critical velocity of runaway electrons, they run away. When the loop voltage becomes negative or near zero, the intensity of hard x-ray emission decays to a very low level.

4. PF coil cut-off after LHW was launched into plasma

Time evolution of the main plasma parameters for the discharge with CRU by LHCD only (No. 25427) and normal ohmic discharge (No. 25395) is shown in figure 9. From figure 9 we can see that 1 MW LHW was launched into plasma to ramp up plasma current at $t_1 = 3018$ ms assisted by ohmic heating. The PF coil cut off at $t_2 = 3058$ ms; under

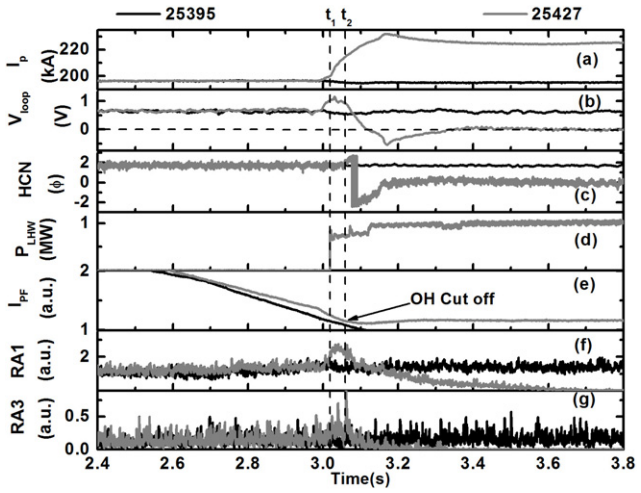

Figure 9. Time evolution of the main plasma parameters for the discharge with CRU by LHCD only (No. 25427) and normal ohmic discharge (No. 25395). From top to bottom: the plasma current (I_P), loop voltage (V_{loop}), far infrared laser interferometer (HCN), LHCD power (P_{LHW}), PF coil current (I_{PF}), hard x-ray emission in 0.1–1.1 MeV detected by the CdTe detector (RA1), hard x-ray emission in 0.5–7.0 MeV detected by the NaI(TL) detector (RA3).

this condition the plasma current is ramped up by a fully non-inductive LHCD only. The plasma current is ramped up in 150 ms (3018–3168 ms) from 200 to 232 kA. The plasma current is maintained stably after a rapid increase. The increase of loop voltage during $t_1 = 3018$ ms and $t_2 = 3058$ ms is induced by the changing of PF coil current as is shown in figure 9. Therefore, the intensity of hard x-ray emission during t_1 and t_2 increases, and then reduces to a low level because of the increase of the electron density n_e and the decrease of the loop voltage.

5. Conclusions

In this paper we investigate the behaviors of runaway electrons in the CRU by LHCD without resistor switches in ohmic heating circuits, as well as the relevant plasma parameters evolving during the CRU phase driving by LHCD with PF coil cut-off on the EAST tokamak. It is found that the runaway electron counts increase when LHW is launched into plasma, and then decrease gradually as the discharge goes on.

During the experiment, LHW was launched into plasma in order to drive plasma current with the solenoidal current flat. The plasma current decays within several milliseconds as a result of the ohmic heating cut-off and ramps up because of the LHCD. A fully non-inductive LHCD is being applied. It is found that the hard x-ray emission produced by fast electron bremsstrahlung decreases because of the decrease of the acceleration by loop voltage produced by plasma current decays when the PF coil current cut off. ECE increases to a high level when LHW was launched into plasma and then decays because of the increased line integral electron density and the negative loop voltage. The H_α line emission (Ha), impurity line emission (UV) and soft x-ray emission increase. Therefore, the plasma radiation loss detected by absolute XUV increases to a very high level because of extensive impurity emission during the CRU by LHW. Also, the MHD activity takes place during the CRU driving by LHCD.

Under the condition of PF coil cut-off before LHW was launched into plasma, the runaway electron counts increase after LHW was launched into plasma, and then decrease gradually as the discharge goes on. The reason is that the positive loop voltage decreases to negative because of ohmic heating cut-off and current decays. And then loop voltage remains about zero when a fully non-inductive LHCD is being applied. Furthermore, the line integral electron density increased after LHW was launched into plasma because of extensive impurity emission. However, under the condition of PF coil cut-off at the same time as LHW was launched into plasma, the intensity of runaway electrons increases after LHW was launched into plasma. The reason is that the loop voltage cannot reduce to zero immediately because of the electromagnetic induction. When the loop voltage becomes negative or near zero, the intensity of runaway electrons decays to a very low level. Under the condition of PF coil cut-off after LHW was launched into plasma, there is an obvious increase of low-energy runaway electrons because of the increase of loop voltage, and then a decrease because of the increase of the electron density n_e and the decrease of the loop voltage.

Acknowledgments

This work has been supported by the National Natural Science Foundation of China (grant numbers 11205029 and 11175045), the Fundamental Research Funds for the Central Universities of China (grant number 12D10915) and the National Magnetic Confinement Fusion Science Program (grant numbers 2009GB106002 and 2009GB107006). The corresponding author is grateful to all members of the EAST Team for their contribution to EAST experiments.

References

[1] Dreicer H 1959 *Phys. Rev.* **115** 238
[2] Dreicer H 1960 *Phys. Rev.* **117** 329
[3] Martín-Solís J R, Sánchez R and Esposito B 2010 *Phys. Rev. Lett.* **105** 185002
[4] Jayakumar R *et al* 1993 *Phys. Lett.* A **172** 447
[5] Bakhtiari M, Kramer G J and Takechi M 2005 *Phys. Rev. Lett.* **94** 215003
[6] Taylor P L *et al* 1996 *Phys. Rev. Lett.* **76** 916
[7] Whyte D G *et al* 1998 *Phys. Rev. Lett.* **81** 4392
[8] Bakhtiari M *et al* 2002 *Nucl. Fusion* **42** 1197
[9] Gill R D *et al* 1993 *Nucl. Fusion* **33** 1613
[10] Gill R D *et al* 2000 *Nucl. Fusion* **40** 163
[11] Imbeaux F, Citrin J and Hobirk J 2011 *Nucl. Fusion* **51** 083026
[12] Jackson G L, Humphreys D A and Hyatt A W 2011 *Nucl. Fusion* **51** 083015
[13] Sips A C C, Casper T A and Doyle E J 2009 *Nucl. Fusion* **49** 085015
[14] Holtkamp N 2008 ITER-IO 2008 the status of the ITER design *Proc. 22nd Int. Conf. on Fusion Energy 2008* (*Geneva, Switzerland*) (*Vienna: IAEA*) CD-ROM file OV/2–1 and www-naweb.iaea.org/napc/physics/FEC/FEC2008/html/index.htm
[15] Bucalossi J *et al* 2008 *Nucl. Fusion* **48** 054005
[16] Wan B *et al* 2009 *Nucl. Fusion* **49** 104011
[17] Bak J S *et al* 2008 Overview of recent commissioning results of KSTAR *Proc. 22nd Int. Conf. on Fusion Energy 2008* (*Geneva, Switzerland*) (*Vienna: IAEA*) CD-ROM file FT/1–1 and www-naweb.iaea.org/napc/physics/FEC/FEC2008/html/index.htm

[18] Fisch N J 1978 *Phys. Rev. Lett.* **41** 873
[19] Fisch N J 1987 *Rev. Mod. Phys.* **59** 175
[20] Bernabei S *et al* 1982 *Phys. Rev. Lett.* **49** 1255
[21] Porkolab M *et al* 1984 *Phys. Rev. Lett.* **53** 450
[22] Fable E, Angioni C and Hobirk J 2011 *Nucl. Fusion* **51** 043006
[23] Gao X, Hu J S and Zhao Y P 2009 *J. Nucl. Mater.* **390** 864
[24] Lu H W, Hu L Q and Chen Z Y 2008 *J. Plasma Phys.* **74** 445
[25] Lu H W, Hu L Q and Lin S Y 2011 *Phys. Scr.* **84** 035503
[26] Esposito B, Bertalot L, Kaschuck Yu A, Portnov D V and Martin-Solis J R 2002 *Nucl. Instrum. Methods* A **476** 522
[27] Esposito B 2003 *Phys. Plasmas* **10** 2350
[28] Martin-Solis J R 2004 *Nucl. Fusion* **44** 974
[29] Esposito B 2002 *Nucl. Instrum. Methods* A **476** 522
[30] Dreicer H 1959 *Phys. Rev.* **115** 238
[31] Kuznetsov Yu K 2004 *Nucl. Fusion* **44** 631
[32] Wesson J 1997 *Tokamak* (Oxford: Oxford University Press) pp 72–5